Removal of ZnO and CuO Nanoparticles from Water Using an Activated Carbon Column

Tropita Piplai[1]; Arun Kumar[2]; and Babu J. Alappat[3]

Abstract: Efficient removal of nanoparticles (NPs) is particularly important in view of the increasing long-term persistence and evidence of considerable ecotoxicity of some nanoparticles. The aim of this study was to understand the effects of flowrate (0.5, 1, and 1.5 mL/min), concentration (1, 10, and 100 mg/L), and the type of nanoparticles (ZnO, CuO, and ZnO + CuO) on the removal of the nanoparticles in an activated carbon column. Flowrate, concentration of NPs, and type of NPs were found to influence the removal at room temperature. Complete removals of both ZnONPs and CuONPs in both single and binary suspensions from water were achieved. Breakthrough was achieved after treating 3 L of water for nearly 50 h for concentrations of 1 and 10 mg/L of ZnONPs and CuONPs. The breakthrough was reached faster for Cu (49.5 h) than Zn (53 h). More work is required to understand the effect of water quality on the removal, to develop methods for quantifying the concentration of nanoparticles after any kind of nanoparticle-water interaction, and to understand the fate and removal mechanism of NPs in the column. **DOI: 10.1061/(ASCE)EE.1943-7870.0001331.** *© 2017 American Society of Civil Engineers.*

Introduction

A rapid increase in the usage of ZnO nanoparticles (NPs) ultimately leads to their growing release into municipal wastewater. CuONPs are used in gas sensors and catalytic processes (Carnes and Klabunde 2003). ZnONPs and metal doped ZnONPs are also being used as photocatalysts for various processes (Sun et al. 2011). Studies suggested that ZnONP concentration was 0.34–1.42 μg/L in treated wastewater in Europe in 2008 (Gottschalk et al. 2009), which increased to 1.7–21 μg/L in 2012 (Tan et al. 2015). Further, occurrence data of CuO are rare and restricted (Mortimer et al. 2010). Considering the rapid and continuous increase in the production and use of these two nanoparticles (Piplai et al. 2017), their environmental concentrations are expected to inevitably increase and are likely to be in the mg/L level in the next few years (Tan et al. 2015). The presence of a mixture of nanoparticles is a more likely scenario in municipal wastewater. Wastewater treatment processes play a crucial role in controlling the entrance of nanoparticles into the environment. Removal of NPs from wastewater treatment plants (WWTPs) using microbes and activated sludge are the only practiced methods as of today (for TiO$_2$ and ZnONP removal).

Based on previous literature studies (Table S1 in Appendix S1), it was evident that the removal of nanoparticles using pure activated carbon (AC) bed columns was not explored. Pure AC indicated that AC was not impregnated with any other compound or metals such as Fe or Ag to enhance the adsorption capacity. It also indicated that

the AC was neither acid washed nor steam activated. These reported studies were considered to select the column parameters for this study. No information and data regarding the removal of mixtures of ZnO and CuO nanoparticles in a column setup using pure AC has been reported to date. Activated carbon has been previously used for water and wastewater treatment. Because adsorptive processes are relatively cost effective, it was worth exploring the removal of nanoparticles by adsorption using AC over sand. No quantitative literature data was available quantifying the amount of NP adsorbed or removed (Ghaedi et al. 2011). Hence, AC was selected as an adsorptive filter media for this study, which was hypothesized to adsorb NPs as well as remove them through filtration. The results of the present analysis were required because batch adsorption isotherms cannot provide accurate scale-up data. This study would be of importance because column operating mode was preferred over batch studies in all industries because the results were better and accounted for all the chemical changes that occurred, which are beyond the scope of batch studies. Column studies are also preferred because the concentration gradient is always maintained, whereas in batch studies, concentration decreases. Hence, column study was preferred to understand the mechanism and apply it at the industrial level.

Thus, the aim of this study was to understand the feasibility of removing nanoparticles from water in an activated carbon-based fixed-bed column. Moreover, information regarding the removal of NPs from water, when present in a binary mixture, might help in adjusting adsorbent dose, reaction time, pH, etc. to obtain the highest removal percentage.

---

[1]Graduate Student, Dept. of Civil Engineering, Indian Institute of Technology Delhi, Hauz Khas, New Delhi 110016, India.

[2]Associate Professor, Dept. of Civil Engineering, Indian Institute of Technology Delhi, Hauz Khas, New Delhi 110016, India (corresponding author). E-mail: arunku@civil.iitd.ac.in

[3]Professor, Dept. of Civil Engineering, Indian Institute of Technology Delhi, Hauz Khas, New Delhi 110016, India.

Methodology

Materials

The AC (CAS Number: 7440-44-0; particle size 0.4–1.68 mm), ZnO nanoparticles (CAS Number: 1314-13-2; particle size < 100 nm), and CuO nanoparticles (CAS Number: 1317-38-0; particle size < 50 nm) were purchased from Sigma Aldrich Corporation (St. Louis, Missouri). These nanoparticles are widely used for

various commercial purposes (Consumer Products Inventory 2015; Gottschalk et al. 2009). Nanoparticles were used as received, and no surface coating treatment was observed (as per provided information sheet) or done on the purchased ZnO and CuO nanoparticles to keep them in suspension. Nanoparticles were spiked in deionized water to make solutions of different concentrations of nanoparticles at neutral pH. This pH was selected because the maximum removal for both ZnO and CuO nanoparticles in binary mixtures (Piplai et al. 2017) was observed at this pH. Secondly, because the pH of drinking water is 7, the study was conducted at this selected pH to also understand the feasibility of removing NPs from drinking water. Deionized water was produced using ELGA LabWater PURELAB Option-Q at resistivity 18.2 $M\Omega \cdot cm$ at 25°C. Brilliant Blue R dye (CAS Number 6104-59-2; dye content ∼50%; technical grade) for conducting the tracer study was purchased from Sigma Aldrich. All chemicals used were of analytical grade and purchased from Merck KGaA (Dermasdat, Germany). Tubing of 4 mm inner diameter was used in this study.

Column Experiments

Using information from Table S1 (Appendix S1), the average diameter of the column was selected to be 1.5 cm, and the length of the column was selected as 15 cm. As seen from Table S1, the transport of Al, Bo, and Cu nanoparticles through sand columns was studied under similar conditions with diameter: height ratio varying between 0.05 and 1, which was assumed to be effective for reactions to occur (Doshi et al. 2008; Jones and Su 2012). Hence, for this study, a diameter:height ratio of 0.1, which gave an internal column diameter of 1.5 cm and length of 15 cm (Fig. 1), was selected.

Flowrates studied were 0.5, 1, and 1.5 mL/min (Torkzaban et al. 2008; Shani et al. 2008), indicating superficial velocities of 4.7×10^{-3} cm/s, 9.4×10^{-3} cm/s, and 14.1×10^{-3} cm/s, respectively. These flowrates were generally maintained through the topsoil and subsurface soil matrix (Godinez and Darnault 2011). The typical flowrate applied was 1 mL/min for nanoparticle movement in a column for a diameter:height ratio between 0.05 and 0.6 (Jones and Su 2012; Godinez and Darnault 2011). A lower and higher flowrate were also applied to study the effect of flowrate on the removal of nanoparticles in the column. Flowrates lower than

0.5 mL/min made it difficult for the solution to pass through the column in an upward direction. Flowrates higher than 1.5 mL/min resulted in flooding of the column and reduced the residence time. Though both upward flow and downward flow have been studied for water treatment in adsorbers, upward flow was preferred because it minimized the channeling effects inside the column (Ghosh and Philip 2005). Moreover, this configuration does not compress the bed in the columns during downward flow (Bohmann et al. 1995).

The column was preconditioned before starting the experiment (Appendix S2). Deionized water at an upward flowrate of 1 mL/min was passed through the column of activated carbon. The pH was maintained at approximately 7–7.2. Effluent pH was measured, and the column was considered pretreated when the pH difference between the influent and effluent was smaller than 0.5 pH units (Gabaldón et al. 2000). For this study, the effluent pH was 6.9 ± 0.4 after the first hour and 7.1 ± 0.3 after the second hour. Hence, the column was considered pretreated.

Tracer Study

The tracer study was done to obtain information on hydrodynamic dispersion coefficient, porosity, and residence time. For the estimation of residence time and porosity, 1 mg/L of Brilliant Blue R dye solution at pH 7 at the lowest flowrate of 0.5 mL/min was passed through the AC column. This flowrate was selected because it helped in estimating the highest residence time, which was fixed as the time duration after which the effluent was collected for the complete analysis. The residence time was measured to be 30 ± 2.3 min for this experiment. This was the time required for the first drop of the dye to be eluted from the column. The tracer experiment was completed when the absorbance value (At) was equal to the initial absorbance (Ao). After the completion of the tracer experiment, pore volume was determined by draining the dye from the column and measuring its volume (Gabaldón et al. 2000). This experiment was repeated thrice. Using this data and the volume of the AC bed used for the experiment, bed porosity (ξ), residence time, and hydrodynamic dispersion coefficient (D_t) were calculated. Descriptions of these calculations are presented in Appendix S3.
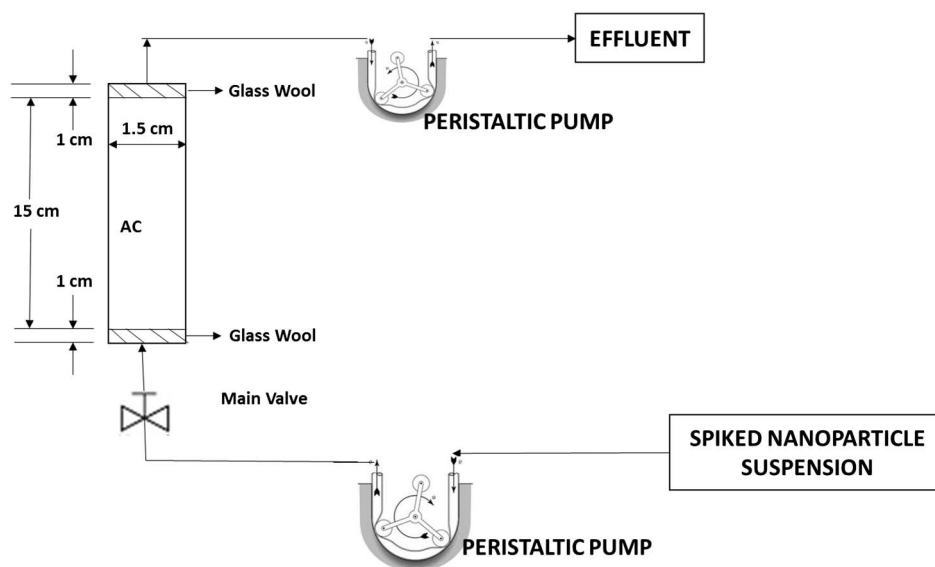

Fig. 1. Schematic representation of the column study

$$\xi = \text{Pore Volume}/\text{Volume of Activated Carbon Bed} \quad (1)$$

The theoretical residence time was calculated using

$$\text{Residence Time Theoretical} = (\text{Pore Volume})/\text{Flowrate} \quad (2)$$

Column Studies for Nanoparticle Removal

Upward flow in column studies was used to ensure the maximum removal of NPs because it resulted in a maximum interaction between the nanoparticles and the AC column bed (Inyang et al. 2013). Solution containing different concentrations of ZnONP and CuONP in single and binary (mixture of ZnONPs and CuONPs) suspensions (1, 10, and 100 mg/L) was pumped into the column till exhaustion. These nanoparticle concentrations were the highest and lowest adsorbent concentrations used in various previously reported studies (Table S1 in Appendix S1) as well as the maximum concentration that has been detected in the environment (Hou et al. 2012; Westerhoff et al. 2011). In the binary suspension, the ratio of both the nanoparticles were taken to be 1:1. The effect of different ratio proportions (i.e., 1:2 and 2:1) on the removal effect of the NPs was studied and discussed in detail in Appendix S8. One column was run without NPs as control. Treated water samples were collected in 50-mL tubes after every 30 min for measuring the remaining concentration of nanoparticles and remaining turbidity (Torkzaban et al. 2008). Experiments were conducted at room temperature ($28°C \pm 2$). The column was run until the effluent turbidity was reported to be equivalent to its initial value, at which point it was assumed that complete exhaustion had been obtained. Column studies were terminated when the column reached exhaustion. The concentration of total Zn and Cu measured in the treated water was used to calculate the removal of nanoparticles from water. Total treated water collected at the end of the experiment, supernatant samples collected after every time interval, and loaded AC collected from the column at the end of the experiment were acid digested as per method 3030 D (APHA 1998) and Hou et al. (2012). Filter papers of 11-μm pore size were used to first filter the acid-digested AC solution before analyzing it for total metal concentration using an atomic absorption spectrophotometer (AAS). Filtration was done to prevent any clogging due to minute particles of activated carbon. Previous studies have also used metal measurements to indicate nanoparticle concentration (Sun et al. 2013; Honda et al. 2014). The range of detection limit of AAS in a liquid state was 0.01–2 mg/L for Zn and 0.04–10 mg/L for Cu.

Turbidity is an indication regarding the clarity of water and is mainly related to the sizes and the number of particles. It can be used as a measuring technique for monitoring the colloidal nanoparticle concentration along the treatment process (Liu et al. 2013). Standard nanoparticle-turbidity and ions-turbidity calibration graphs were plotted between measured turbidity and known concentration of ZnONPs and Zn ions (from ZnCl$_2$) [Fig. 2(a)], CuONPs and Cu ions (from CuSO$_4 \cdot$ 5H$_2$O) [Fig. 2(b)], and mixture suspension (ZnONPs + CuONPs and Zn ions + Cu ions) [Fig. 2(c)] to predict the mass concentrations of ions remaining in the supernatant.

Based on the turbidity readings for the total ZnO and CuO nanoparticles for a specific time duration, the C/Co graph was plotted with respect to time. Total nanoparticles removed and the adsorption capacities of AC were calculated (Zeng 2004). These adsorption capacities of AC in terms of total Zn and Cu adsorbed on AC were reported in metal mg/g, which reported the total column adsorption data.

Breakthrough Curve Analysis

The performance of a fixed-bed column in removing nanoparticles from water was described through the concept of breakthrough curve analysis. The time to reach the breakthrough point and the shape of the breakthrough curve were very important characteristics for determining the operation and the dynamic responses of a fixed-bed column.

To design the nanoparticle removal process in the column, it was necessary to predict the breakthrough curve or concentration-time profile of the AC for the nanoparticles under the given set of operating conditions. A Thomas model, Yoon-Nelson model and Bohart-Adams kinetic model were used in this study to analyze the breakthrough curve of the selected AC-NP system. These models have been previously used for predicting the breakthrough curves for industrial dyes and metal ions in a column study (Han et al. 2008). Their detailed description and usage are provided in Appendix S4. These analyses provided information on the rate constant, breakthrough curves, and adsorptive capacity of the adsorbent, which were useful in describing and predicting the column adsorptions and providing information regarding the design of a column adsorption system.

Particle Removal

Head loss was calculated to account for the changes in the flowrate (Appendix S5). For this study, the flow was randomly distributed around the AC particle surface and not in a straight line leading to collisions between AC and NPs. These collisions might have resulted in adsorption of the particles and trapping of the nanoparticles in the voids between the AC particles. Hence, it was hypothesized that the nanoparticles were removed from the water by both
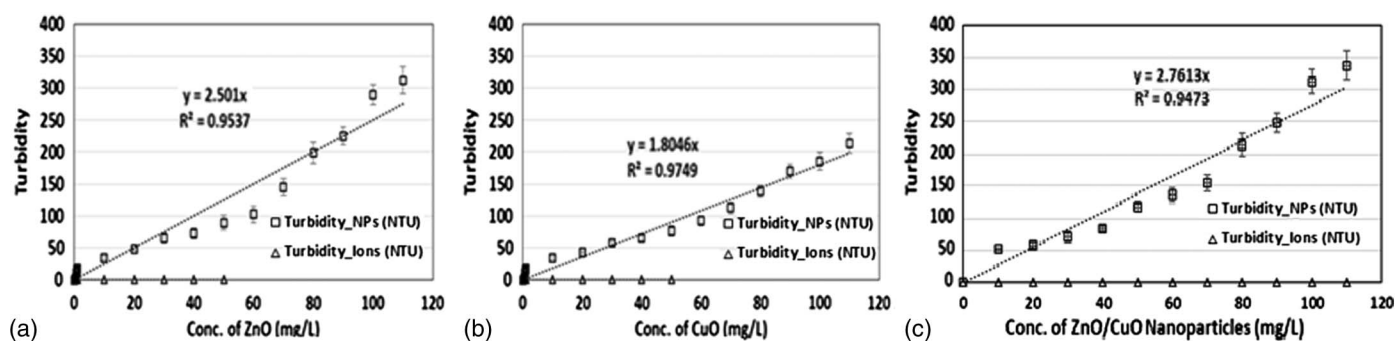

Fig. 2. Concentration versus turbidity: (a) ZnO nanoparticles and Zn^{2+} ions; (b) CuO nanoparticles and Cu^{2+} ions; (c) ZnO + CuO nanoparticles and Zn^{2+} + Cu^{2+} ions (triplicate study; error bars indicate the standard error of the mean variation value for the triplicate study reported)

adsorption and filtration inside the column. Thus, filtration parameters such as attachment efficiency (α_{pc}), NP deposition rate (k_d), and filter coefficient (λ) were calculated to predict and understand the collision-attachment efficiency and collector-attachment efficiency of nanoparticles through the AC filter bed using the clean-bed filtration theory. A detailed description is presented in Appendix S6.

Samples were also analyzed for understanding surface morphology using transmission electron microscopy (TEM) and energy-dispersive X-ray spectroscopy (EDS) for confirming the deposition of Zn and Cu onto AC (qualitatively) and for estimating the particle size in water using dynamic scattering light (DLS). A detailed analysis and inference are provided in Appendix S9.

Statistical Methodology

The normality test of adsorbed Zn (mg Zn/g AC) and adsorbed Cu (mg Cu/g AC) was done using the Shapiro-Wilk test in *Minitab*. All values were found to be normally distributed. For every experimental combination, an ANOVA two-factor model was applied to test the significance of the flowrate and the concentration of nanoparticles on the type of nanoparticle for a test with level of significance $\alpha = 0.05$ (Devore 2004).

Results and Discussion

Tracer Study

Residence time (experimental) was noted to be 30 ± 2.8 min for the lowest flowrate of 0.5 mL/min. This was the time taken for the first drop to be eluted from the column. Residence time (theoretical) was calculated using Eq. (1) for flowrates 0.5, 1, and 1.5 mL/min and were found to be 21.6 min (30 ± 2.8 min experimental value), 10.8 min, and 7.2 min, respectively.

The hydrodynamic dispersion coefficient was calculated from the plot between M_t/M_o and $t^{1/2}$ (Fig. S1 in Appendix S3). The results showed that value of 2.86×10^{-6} m^2/s [using Eq. (S2) in Appendix S3]. Studies have reported a hydrodynamic dispersion coefficient of approximately 1.52×10^{-5} m^2/s to 5×10^{-6} m^2/s for the activated bed column (Gabaldón et al. 2000; Drazer et al. 1999). The value in this study was found to lie within this range. Void volume was calculated to be 10.8 ± 1.6 mL and was used to calculate the bed porosity as per Eq. (1). The bed

porosity was calculated to be 0.69. The bed porosity of the AC bed, as seen in previous studies (Table S1 in Appendix S1), was approximately 0.725 (Gabaldón et al. 2000).

Removal of Nanoparticles in an Activated Carbon Bed Column

A standard graph was plotted between measured turbidity and known concentrations of ZnO nanoparticles [Fig. 2(a)] and CuO nanoparticles [Fig. 2(b)] to predict the mass concentration of remaining nanoparticles in the supernatant. The turbidity for the same concentration of Zn ions and Cu ions were measured to incorporate the turbidity contribution from ions. A linear model passing through the origin was fitted for each case.

Breakthrough curves were plotted (Figs. 3 and 4) using the ZnO nanoparticle and CuO nanoparticle present in the supernatant using the turbidity calibration curve. A standard graph was plotted between the measured turbidity and the known concentrations of ZnONPs and CuONPs to estimate the concentrations of particles eluted by the column. Turbidity of the sample collected was measured after every time interval using a turbidity meter (2100P, HACH, Loveland, Colorado) to estimate the concentration of ZnO and CuO nanoparticles in the treated water.

For NP Concentration = 1 mg/L

Figs. 3 and 4 indicate the breakthrough curves for ZnO and CuO nanoparticles (at Co = 1 mg/L) for three flowrates (0.5, 1, and 1.5 mL/min) in single and binary suspensions.

During the passing of 1 mg/L ZnO nanoparticle suspension through the AC column, the time-to-breakthrough values were found to be 53 ± 1.8, 55.5 ± 2.3, and 49 ± 0.8 (average $\pm$ standard deviation) hours for flowrates 0.5, 1, and 1.5 mL/min, respectively. The two-way ANOVA with replication for two-factor analysis described the effect of the concentration (p value = 0.0011) and flowrate (p value = 0.0006) and their interaction (p value = 0.0241888) for ZnO (single) on the C/Co plot versus time.

During the passing of 1 mg/L of CuO nanoparticle suspension through the AC column, the time-to-breakthrough values were found to be 49.5 ± 1.6 h, 53 ± 1.2 h, and 47 ± 1.8 h for flowrates 0.5, 1, and 1.5 mL/min, respectively. The two-way ANOVA with replication for two-factor analysis described the effect of the concentration (p value = 0.00235) and flowrate (p value = 0.0008)

Fig. 3. Breakthrough curves during passing ZnO nanoparticles to AC column: (a) single NP case; (b) binary suspension at three flowrates [at nanoparticle concentration 1 mg/L for both cases; 0.5 mL/min indicates data obtained at this flowrate; 0.5 mL/min (model) indicates best model (Thomas) describing the observed data at this flowrate]
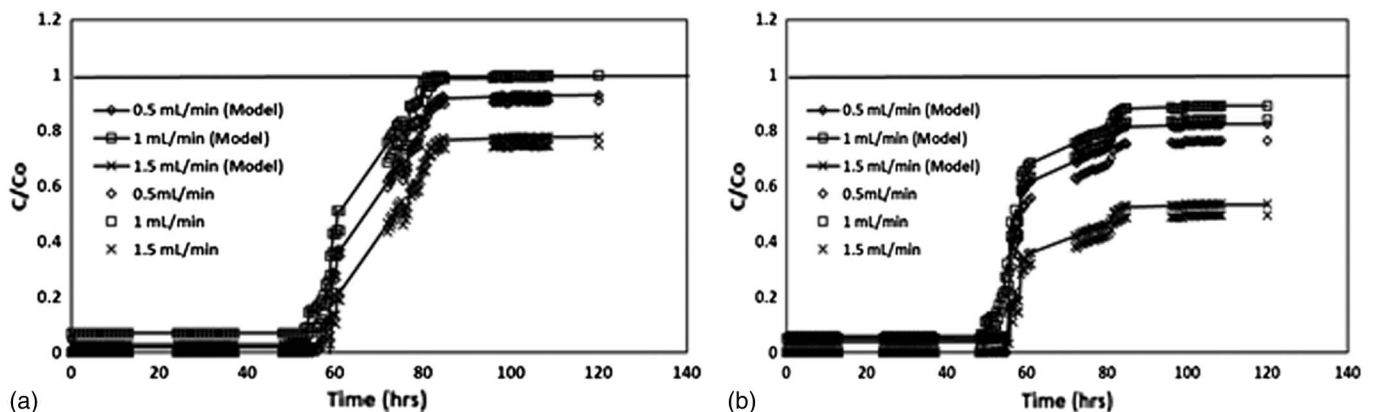
Fig. 4. Breakthrough curves during passing CuO nanoparticles to AC column: (a) single NP case; (b) binary suspension at three flowrates [at nanoparticle concentration 1 mg/L for both cases; 0.5 mL/min indicates data obtained at this flowrate; 0.5 mL/min (model) indicates best model (Thomas) describing the observed data at this flowrate]
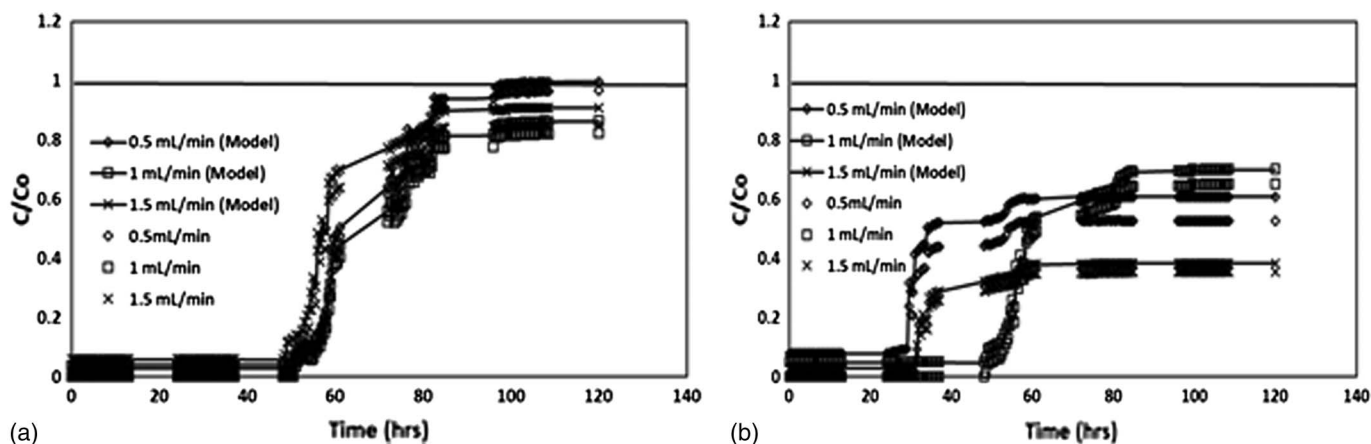
and their interaction (p value = 0.0352) for CuO (single) on the C/C_o plot versus time.

However, during the passing of binary suspension through the AC column, the time-to-breakthrough values for ZnO nanoparticles were reduced to 48.5 ± 1.8 h, 49 ± 2.6 h, and 45.5 ± 1.9 h for the three selected flowrates 0.5, 1, and 1.5 mL/min, respectively. The times to breakthrough for CuO nanoparticles were reduced to 43 ± 1.7 h, 48.5 ± 2.7 h, and 43.5 ± 1.4 h for the three selected flowrates 0.5, 1, and 1.5 mL/min, respectively.

For both nanoparticles, it was observed that the time to breakthrough reduced when the nanoparticles were passed in mixture solution compared to when the nanoparticles were passed separately.

Tables 1–3 show the time to breakthrough for all conditions studied. Breakthrough curves for all other cases are presented in Appendix S7.

The breakthrough was reached earlier for total CuO than for ZnO. The time to reach the complete saturation point was also faster for CuO than ZnO.

Thus, as shown in Appendix S7 (Figs. S4–S7), for ZnONPs, the AC bed column removed the nanoparticles to less than the permissible limit (less than 5 mg/L) for as long as 75–80 h and 60 h for single and binary suspensions, respectively, and for CuONPs, the AC bed removed the nanoparticles to less than the permissible limit (less than 1 mg/L) for as long as 60 and 50 h for single and binary suspensions, respectively.

Table 1. Filtration Parameters for ZnO and CuO Nanoparticles at $C_o = 1$ mg/L Nanoparticle Concentration

Parameter	Flowrate = 0.5 mL/min				Flowrate = 1 mL/min				Flowrate = 1.5 mL/min			
	ZnO	CuO	ZnO (M)	CuO (M)	ZnO	CuO	ZnO (M)	CuO (M)	ZnO	CuO	ZnO (M)	CuO (M)
η_{filter}	0.99	0.99	0.99	0.99	0.99	0.99	0.99	0.99	0.99	0.99	0.99	0.99
η_0	0.09	0.10	0.09	0.10	0.09	0.10	0.09	0.10	0.09	0.10	0.09	0.10
Breakthrough time (h)	53	49.5	48.5	43	55.5	53	49	48.5	49	47	45.5	43.5
t for C/C_o max (h)	100	96	98	92.5	107.5	103	101.5	98.5	86.5	84.5	81.5	79.5
Metal adsorbed (mg/g)	4.15	4.78	3.12	4.6	4.96	5.13	4.32	4.78	1.8	2.38	1.03	1.51
α	5.6	6.2	3.7	4.8	6.1	6.7	5.4	5.9	4.8	5.2	3.1	3.7
NP deposition rate coefficient (K_d) (h^{-1})	0.002	0.0038	0.00165	0.0020	0.00352	0.00412	0.00249	0.00331	0.0021	0.0024	0.00128	0.00139
Filter coefficient (λ) (cm^{-1})	0.65	0.72	0.52	0.59	0.78	0.82	0.65	0.68	0.56	0.57	0.43	0.48

Table 2. Filtration Parameters for ZnO and CuO Nanoparticles at $C_o = 10$ mg/L Nanoparticle Concentration

Parameter	Flowrate = 0.5 mL/min				Flowrate = 1 mL/min				Flowrate = 1.5 mL/min			
	ZnO	CuO	ZnO (M)	CuO (M)	ZnO	CuO	ZnO (M)	CuO (M)	ZnO	CuO	ZnO (M)	CuO (M)
η_{filter}	0.99	0.99	0.99	0.99	0.99	0.99	0.99	0.99	0.99	0.99	0.99	0.99
η_0	0.05	0.06	0.05	0.06	0.05	0.06	0.05	0.06	0.05	0.06	0.05	0.06
Breakthrough time (h)	39	37	25	23.5	48	47.5	36.5	32.5	53	50.5	48.5	42.5
t for C/C_o max (h)	76.5	73	71	68.5	105.5	100.5	98.5	94.5	67	58	81.5	53.5
Metal adsorbed (mg/g)	36.5	45.1	21.3	34.8	48.7	53.6	41.3	46.2	21.3	29.6	9.87	14.8
α	5.9	6.5	3.9	4.9	6.5	7.2	5.2	5.6	4.7	4.9	3.4	3.8
NP deposition rate coefficient (K_d) (h^{-1})	0.005	0.007	0.004	0.0025	0.0036	0.00457	0.00252	0.00351	0.0019	0.0021	0.0011	0.0012
Filter coefficient (λ) (cm^{-1})	0.72	0.81	0.64	0.69	0.83	0.86	0.67	0.70	0.54	0.56	0.48	0.45

Table 3. Filtration Parameters for ZnO and CuO Nanoparticles at $C_o = 100$ mg/L Nanoparticle Concentration

Parameter	Flowrate = 0.5 mL/min				Flowrate = 1 mL/min				Flowrate = 1.5 mL/min			
	ZnO	CuO	ZnO (M)	CuO (M)	ZnO	CuO	ZnO (M)	CuO (M)	ZnO	CuO	ZnO (M)	CuO (M)
η_{filter}	0.99	0.99	0.99	0.99	0.99	0.99	0.99	0.99	0.99	0.99	0.99	0.99
η_0	0.03	0.04	0.03	0.04	0.03	0.04	0.03	0.04	0.03	0.04	0.03	0.04
Breakthrough time (h)	27	23.5	24.5	19.5	49.5	43.5	46.5	38.5	42	21.5	39.5	17.5
t for C/C_o max (h)	73.5	69	67	64.5	101.5	97.5	94.5	89.5	82.5	54.5	79.5	49
Metal adsorbed (mg/g)	279.2	298.7	206.5	214.6	317.6	345.6	246.5	287.9	246.3	276.8	71.8	91.7
α	3.8	4.1	3.2	3.4	4.7	4.9	3.6	3.8	3.2	3.4	2.7	2.9
NP deposition rate coefficient (K_d) (h^{-1})	0.0012	0.003	0.001	0.002	0.001	0.003	0.001	0.002	0.002	0.003	7.9×10^{-4}	8.7×10^{-4}
Filter coefficient (λ) (cm^{-1})	0.47	0.51	0.35	0.30	0.53	0.57	0.46	0.48	0.27	0.29	0.16	0.18

The two-way ANOVA analysis indicated that the effect of concentration of nanoparticles and flowrates were significantly different (i.e., $p < 0.05$) for both single and binary suspensions. Moreover, the interaction of these parameters was also significantly different (i.e., $p < 0.05$). Thus, this data indicated that the removal of nanoparticles in the column was dependent on all the factors as well as on the interaction between these parameters. The observed time interval between ZnO and CuO nanoparticle breakthroughs was quite short.

The two metal sorptions resulted in CuO breaking through the column earlier than ZnO because of its low affinity. The sharp favorable CuO breakthrough curve can be explained by the higher affinity of Cu toward the AC bed than that of Zn (Huheey 1978). Because of this higher affinity, CuO attaches onto AC better than ZnO because the functional groups on the surface of AC bind better with Cu than Zn (Babel and Kurniawan 2004). An overshoot of the ZnO exit concentration was observed and explained by the electrostatic attraction between CuO and AC and ZnO and AC (Piplai et al. 2017). The same effect was observed for CuO to a lesser extent than ZnO. The time interval between ZnO and CuO nanoparticle breakthroughs was also quite short.

Breakthrough Curve Modeling

The dynamic behaviors of the ZnO and CuO nanoparticles onto AC were predicted with the Bohart-Adams, Thomas, and Yoon-Nelson models. Out of the three mathematical models tested for predicting the breakthrough curves for ZnO and CuO nanoparticles (single and binary suspensions) from the AC column, the linear regression coefficient values were comparatively better ($R^2 > 0.9$) for the Thomas model than the Bohart-Adams and Yoon-Nelson models. The Thomas model was found suitable to describe the data for both Zn and Cu in single and binary suspensions (Fig. S2 in Appendix S4). The Bohart-Adams model described only the initial part of the curve of breakthrough in accordance with the made approximation ($C \ll C_o$). Hence, this model was not suitable for this study. It was also observed from the data summarized in Table 4 that the q_e values calculated from the Thomas model were very close to the experimentally obtained values listed in Tables 1–3. These values increased with flowrate up to the optimum flowrate and then decreased.

The Thomas model was suitable for adsorption processes in which the external and internal diffusions will not be the limiting step that has been reported previously in this study (Ayoob and Gupta 2007). The various model parameters are reported in Table 4.

The Thomas rate constant, as seen in Table 4, decreased with the increase in influent NP concentration and increased with the increase in flowrate. This trend was in agreement with the previous literature studies reported for the removal of dyes and metal ions in column studies (Xu et al. 2013; Ayoob and Gupta 2007). This can be attributed to the fact that the driving force for adsorption is mainly the concentration difference between the nanoparticles on AC and the nanoparticles in the solution (Aksu and Gonen 2004). Further studies are required to establish this mechanism in detail.

Single Collector and Attachment Efficiency Filtration Model

A conceptual view of the three mechanisms proposed by Yao (1971), Rajagopalan and Tien (1976), and Tufenkji and Elimelech (2004) have presented models for long-range transport of particles through the media grain (AC) that are included in the calculation

Table 4. Kinetic Model Parameters for Different Conditions for Thomas Model

Parameter	Zn (single)			Cu (single)			Zn (binary)			Cu (binary)		
	K (L/mg/h)	q_e (mg/g)	R^2	K (L/mg/min)	q_e (mg/g)	R_2	K (L/mg/min)	q_e (mg/g)	R_2	K (L/mg/min)	q_e (mg/g)	R_2
Flowrate = 0.5 mL/min												
1 mg/L	0.078	2.2	0.926	0.081	5.35	0.928	0.065	3.12	0.959	0.07	4.63	0.916
10 mg/L	0.073	38.9	0.916	0.076	47.2	0.901	0.061	21.3	0.933	0.06	39.2	0.990
100 mg/L	0.025	282.1	0.958	0.020	314.2	0.985	0.018	243.6	0.941	0.02	273	0.958
Flowrate = 1 mL/min												
1 mg/L	0.093	4.72	0.969	0.094	5.27	0.936	0.082	3.8	0.941	0.08	4.1	0.969
10 mg/L	0.086	44.6	0.969	0.089	56.2	0.979	0.073	38.7	0.970	0.07	41.8	0.907
100 mg/L	0.045	389.7	0.979	0.048	426.8	0.899	0.038	342.8	0.922	0.04	377	0.918
Flowrate = 1.5 mL/min												
1 mg/L	0.13	1.82	0.907	0.18	2.37	0.919	0.09	1.03	0.934	0.11	1.51	0.928
10 mg/L	0.10	24.5	0.918	0.16	33.2	0.973	0.08	11.3	0.946	0.10	20.6	0.918
100 mg/L	0.08	216.3	0.897	0.10	286.7	0.919	0.07	195.6	0.977	0.09	223	0.938

of the single collector efficiency (η_0). The three mechanisms considered (Appendix S6) for long-range transport of particles to a media collector are interception, sedimentation, and Brownian motion (Benjamin and Lawler 2013).

The Tufenkji and Elimelech model (Tufenkji and Elimelech 2004) included particle diffusion (Brownian motion) within the context of the flow regime so that all three long-range transport mechanisms were considered simultaneously for laminar conditions only (Fig. S3 in Appendix S6). In this study, the Reynolds numbers calculated [Appendix S5 and Eq. (S6)] were found to be 4.43, 8.87, and 13.30 for flowrates 0.5, 1, and 1.5 mL/min, respectively (for laminar flow, $N_{Re} < 2,300$). From Tables 1–3, the various filtration parameters were calculated for different superficial velocities and recorded for different nanoparticle concentrations for both single and binary suspensions. All calculations were done at the breakthrough point.

The head loss was measured to be 0.006, 0.013, and 0.02 cm for selected flowrates 0.5, 1, and 1.5 mL/min, respectively [Appendix S5 and Eq. (S7)]. The filtration parameters, such as attachment efficiency (α_{pc}), NP deposition rate (k_d), and filter coefficient (λ), were calculated [Appendix S6 and Eqs. (S11)–(S13)]. The effects of the initial nanoparticle concentrations (1, 10, and 100 mg/L) on the removal process for the different flowrates and fixed bed height of 15 cm are shown in Tables 1–3.

Factors Affecting the Removal of Nanoparticles from Water

Effect of Nanoparticle Concentration

From Tables 1–3, it was concluded that the breakthrough time was reached faster for CuO than ZnO in both single and binary suspensions at all three concentrations (i.e., 1, 10, and 100 mg/L). Comparatively, the fastest to reach the breakthrough time was at a concentration 100 mg/L, followed by 10 mg/L and then 1 mg/L. Similarly, the time to reach C/C_o (max) was also faster for CuO than ZnO in both single and binary suspensions at concentration 100 mg/L, followed by 10 mg/L and then 1 mg/L. It can be deduced that, at lower inlet concentrations, both a slower breakthrough curve and the highest treated volume were obtained. The AC bed column works best for nanoparticle concentrations of 1 and 10 mg/L; however, the adsorption capacity decreased sharply as the concentration increased from 10 to 100 mg/L. These results were due to the overlapping of the adsorption sites because of overcrowding of adsorbent particles and an increase in diffusion path length (Shukla et al. 2002). The attachment coefficient was the highest at concentrations 1 and 10 mg/L for both ZnO and CuO. Both the filter coefficient and the rate of deposition were the highest at NP concentrations of 1 and 10 mg/L and lowest for 100 mg/L for both ZnONPs and CuONPs. Thus, it was concluded from the above findings that the concentrations of 1 and 10 mg/L of ZnONPs and CuONPs worked favorably in removing nanoparticles using the AC bed column from water at pH 7. The effects of proportion of concentration of the nanoparticles in binary suspension were studied in detail. The results are presented and discussed in Appendix S8.

Effect of Superficial Velocity

From Tables 1–3, the effect of superficial velocities (4.7×10^{-3} cm/s, 9.4×10^{-3} cm/s, and 14.1×10^{-3} cm/s) was also studied. It was reported from the findings of this paper that the breakthrough time was reached fastest at velocity 4.7×10^{-3} cm/s, followed by 9.4×10^{-3} cm/s and then 14.1×10^{-3} cm/s. Similarly, the time to reach C/Co (max) was also faster for CuO than ZnO in both single and binary suspensions at velocity 4.7×10^{-3} cm/s, followed by 9.4×10^{-3} cm/s and then 14.1×10^{-3} cm/s.

The attachment coefficient was the highest for superficial velocities 4.7×10^{-3} cm/s and 9.4×10^{-3} cm/s for both ZnONPs and CuONPs. Both the filter coefficient and the rate of deposition were the highest at velocity 4.7×10^{-3} cm/s, followed by 9.4×10^{-3} cm/s and then 14.1×10^{-3} cm/s for both the nanoparticles.

This trend implies that with an increase in superficial velocity, there was a decrease in residence time, leading to lesser interaction between the nanoparticles and AC. Thus, it was concluded from the above findings that the superficial velocities 4.7×10^{-3} cm/s and 9.4×10^{-3} cm/s for the AC bed column worked favorably in removing these nanoparticles from water at pH 7.

Effect of Type of Nanoparticle

The breakthrough was reached faster for CuONPs than ZnONPs in both single and binary suspensions (as reported in Table 4 through rate constant K_{thomas}). Similarly, the time to reach C/C_o (max) was also faster for CuO than ZnO in both single and binary suspensions. The time to breakthrough and time to reach C/C_o (max) were faster for single suspensions than binary suspensions. The attachment coefficient was higher for CuONPs than ZnONPs in single suspensions than in binary suspensions (Tables 1–3). Both the filter coefficient and the rate of deposition were higher for CuONPs than ZnONPs in single suspensions than in binary suspensions. It was also inferred that CuONPs were removed better than ZnONPs by the AC bed column at neutral pH. As seen previously, all these parameters were better in single suspensions than binary suspensions. Kouakou et al. (2013) stated that the competitive adsorption followed the sequence Pb > Cu > Fe > Zn for activated carbon. Thus, the removal of Zn was reduced in comparison with that of Cu for the same time duration, as was seen from this study. The concentration of Cu was also reduced because of the presence of Zn (at a reduced extent). The slow transport of ZnO and CuO at lower concentrations onto AC was due to the lower concentration gradient resulting in a slower breakthrough curve. Both the filter coefficient and the rate of deposition were higher for CuONPs than ZnONPs in single suspensions than in binary suspensions. Moreover, as shown in Tables 1–3, the removal of CuONPs was higher than that of ZnONPs. Thus, it was hypothesized that the affinity toward CuONPs was more than ZnONPs as observed in the case of free metals and AC. Additionally, the Cu ions that dissociated from CuONPs had a lower ionic size, lower tendency to hydrolyze, and higher binding energy, which increased its affinity toward AC compared to that of Zn ions dissociated from ZnONPs (Piplai et al. 2017).

Comparison with Previously Reported Studies of Filtration Parameters for Different Nanoparticles in a Column Study

A comparative study was done, and no available study was reported in literature for nanoparticle adsorption on pure AC bed columns. Studies reporting filtration parameters (Table S2 in Appendix S10) for different nanoparticles in a column study were studied. The η_o (collector efficiency) for different nanoparticles varied between $2.5 \times 10^{-3} - 0.095$, whereas the η_o (collector efficiency) for ZnO and CuO nanoparticles in this study were reported to be 0.008–0.017 and 0.09–0.021, correspondingly. The efficiency was low for sand, whereas in this study, it was slightly higher because the collector used here was AC, which had higher collecting

efficiency than sand because the porosity of sand was reported in literature to be 0.25–0.3 and AC was 0.68. Moreover, this data correlated with the proposed mechanism, which reported that AC had more preference for Cu than Zn. The attachment efficiencies for both nanoparticles in this study, i.e., 6.5 (ZnONPs) and 7.2 (CuONPs), were comparable with the other nanoparticles reported (Table S2 in Appendix S10). The variation in attachment efficiency might be due to various properties, such as the size of the collector (sand or activated carbon), size of the nanoparticles, or length of the column. Attachment efficiency decreases as nanoparticle size increases because the small particles diffuse faster than the large ones (Shen et al. 2010). In this study, it was noted that the nanoparticle size was approximately 90 nm, whereas the previous studies reported the nanoparticle diameter to be less than 20 nm. Hence, this can be attributed as a major factor that resulted in low attachment efficiencies. Moreover, as the collector diameter (i.e., activated carbon in this case) increases, the attachment efficiency increases (Torkzaban et al. 2008). The collector diameter for this study was reported to be 0.104 cm, whereas the previous studies reported it (Table S2 in Appendix S10) to be approximately 100 μm. The ZnO and CuO nanoparticle deposition rate on AC ranged between 0.005 and 0.001 h^{-1}. The deposition rates reported in literature varied within a huge range, and the experimental data of the present study was within this range. The lowest deposition rate was as low as $1–2.3 \times 10^{-4}$ h^{-1} to as high as 156 h^{-1} for TiO$_2$NPs. For ZnONPs, it was reported for this study to be 3.40 h^{-1}, which was higher than the values reported in the present study, though for CuONPs, the deposition rate reported was within the experimental data range.

Summary and Conclusions

1. This study helped in understanding the performance modeling of the filter and attachment efficiency of ZnO and CuO nanoparticles in an AC bed column. A 90% removal of ZnONP and CuONP from the AC bed column was observed. Flowrates and concentrations of NPs were found to influence the removal at room temperature. Complete removals of both ZnONP and CuONP for both single and binary suspensions from water in the AC column were achieved and sustained for nearly 50 h for concentrations of 1 and 10 mg/L of ZnONPs and CuONPs before the breakthrough was reported.
2. At a nanoparticle concentration of 1 mg/L, for single suspension, for ZnO nanoparticles, the times to breakthrough were found to be 53, 55.5, and 49 h, and for CuO nanoparticles, they were found to be 49.5, 53, and 47 h for flowrates 0.5, 1, and 1.5 mL/min, respectively. The times to reach C/C_o (max), i.e., 1, for ZnO nanoparticles were 100, 107.5, and 86.5 h, and for CuO nanoparticles, 96, 103, and 84.5 h for flowrates 0.5, 1, and 1.5 mL/min, respectively.
3. Similarly, for binary suspensions, for ZnO nanoparticles, the times to breakthrough were found to be 48.5, 49, and 45.5 h, and for CuO nanoparticles, they were found to be 43, 48.5, and 43.5 h for flowrates 0.5, 1, and 1.5 mL/min, respectively. The times to reach C/C_o (max), i.e., 1, for ZnO nanoparticles were 98, 101.5, and 81.5 h, and for CuO nanoparticles, 92.5, 98.5, and 79.5 h for flowrates 0.5, 1, and 1.5 mL/min, respectively. ANOVA model statistical tools were applied, and data were analyzed.
4. The filtration parameters, such as attachment efficiency (α_{pc}), NP deposition rate (k_d), and filter coefficient (λ), were calculated. Based on these parameters, it was concluded that the concentrations of 1 and 10 mg/L and superficial velocities of

4.7×10^{-3} cm/s and 9.4×10^{-3} cm/s worked favorably for the AC bed column in removing both the nanoparticles from water at pH 7. It was also concluded that Cu was removed better than Zn by the AC bed column at neutral pH.

There were no quantitative data available regarding the removal of ZnO and CuO nanoparticles from water, and means of quantifying the concentration of nanoparticles in water should be introduced after any kind of nanoparticle-water interaction. Removal of nanoparticles using an AC bed filter as a polishing unit may result in enhanced removal of these nanoparticles. Overall, this study indicated that AC can be used as an efficient adsorbent filter for removing ZnO and CuO nanoparticles (single and mixture) from water.

Acknowledgments

Supplemental Data

Appendixes S1–S10 (consisting of Figs. S1–S11 and Tables S1 and S2) are available online in the ASCE Library (www.ascelibrary.org).

References

Aksu, Z., and Gonen, F. (2004). "Biosorption of phenol by immobilized activated sludge in a continuous packed bed: Prediction of breakthrough curves." *Process Biochem.*, 39(5), 599–613.

APHA (American Public Health Association). (1998). *Standard methods for the examination of water and wastewater*, 20th Ed., Public Health Association, Washington, DC, 3:6–3:10.

Ayoob, S., and Gupta, A. K. (2007). "Sorptive response profile of an adsorbent in the defluoridation of drinking water." *Chem. Eng. J.*, 133(1–3), 273–281.

Babel, S., and Kurniawan, T. A. (2004). "Cr(VI) removal from synthetic wastewater using coconut shell charcoal and commercial activated carbon modified with oxidizing agents and/or chitosan." *Chemosphere*, 54(7), 951–967.

Benjamin, M. M., and Lawler, D. F. (2013). *Water quality engineering: Physical/chemical treatment processes*, Wiley, Hoboken, NJ, 677–720.

Bohmann, A., Pörtner, R., and Märkl, H. (1995). "Performance of a membrane-dialysis bioreactor with a radial-flow fixed bed for the cultivation of a hybridoma cell line." *Appl.–Microbiol. Biotechnol.*, 43(5), 772–780.

Carnes, L. C., and Klabunde, K. J. (2003). "The catalytic methanol synthesis over nanoparticle metal oxide catalysts." *J. Mol. Catal. A*, 194(1–2), 227–236.

Consumer Products Inventory. (2015). "The project on emerging nanotechnologies." Woodrow Wilson International Center for Scholars, Washington, DC.

Devore, L. J. (2004). *Probability and statistics for engineering and the science*, 6th Ed., Thomson Learning, Boston, 441–465.

Doshi, R., Braida, W., Christodoulatos, C., Wazne, M., and O'Connor, G. (2008). "Nano-aluminum: Transport through sand columns and environmental effects on plants and soil communities." *Environ. Res.*, 106(3), 296–303.

Drazer, G., Chertcoff, R., Bruno, L., Rosen, M., and Hulin, J. P. (1999). "Tracer dispersion in packings of porous activated carbon grains." *Chem. Eng. Sci.*, 54(19), 4137–4144.

Gabaldón, C., Marzal, P., Seco, A., and Gonzalez, J. A. (2000). "Cadmium and copper removal by a granular activated carbon in laboratory column

systems cadmium and copper removal by a granular activated carbon in laboratory column systems." *Sep. Sci. Technol.*, 35(7), 1039–1053.

Ghaedi, M., Ramazani, S., and Roosta, M. (2011). "Gold nanoparticle loaded activated carbon as novel adsorbent for the removal of Congo red." *Indian J. Sci. Technol.*, 4(10), 1208–1217.

Ghosh, P. K., and Philip, L. (2005). "Performance evaluation of waste activated carbon on Atrazine removal from contaminated water." *J. Environ. Sci. Health Part B*, 40(3), 425–441.

Godinez, I. G., and Darnault, C. J. G. (2011). "Aggregation and transport of nano-TiO2 in saturated porous media: Effects of pH, surfactants and flow velocity." *Water Res.*, 45(2), 839–851.

Gottschalk, F., Sondere, T., Schols, R., and Nowack, B. (2009). "Modeled environmental concentrations of engineered nanomaterials for different regions." *Environ. Sci. Technol.*, 43(24), 9216–9222.

Han, R., et al. (2008). "Use of rice husk for the adsorption of Congo red from aqueous solution in column mode." *Bioresour. Technol.*, 99(8), 2938–2946.

Honda, R. J., Keeve, V., Daniels, L., and Walker, S. L. (2014). "Removal of TiO$_2$ nanoparticles during primary water treatment: Role of coagulant type, dose, and nanoparticle concentration." *Environ. Eng. Sci.*, 31(3), 127–134.

Hou, L., Xia, J., Li, K., Chen, J., Wu, X., and Li, X. (2012). "Removal of ZnO nanoparticles in simulated wastewater treatment processes and its effects on COD and NH$_4^+$-N reduction." *Water Sci. Technol.*, 67(2), 254–260.

Huheey, J. E. (1978). *Inorganic chemistry: Principles of structure and reactivity*, Harper International Ed., Pearson Education, New York.

Inyang, M., Gao, B., Wu, L., Yao, Y., Zhang, M., and Liu, L. (2013). "Filtration of engineered nanoparticles in carbon-based fixed bed columns." *Chem. Eng. J.*, 220(2013), 221–227.

Jones, E. H., and Su, C. (2012). "Fate and transport of elemental copper (Cu^0) nanoparticles through saturated porous media in the presence of organic materials." *Water Res.*, 46(7), 2445–2456.

Kouakou, U., Ello, A. S., Yapo, J. A., and Trokourey, A. (2013). "Adsorption of iron and zinc on commercial activated carbon." *J. Environ. Chem. Ecotoxicol.*, 5(6), 168–171.

Liu, Y., Tourbin, M., Guiraud, P., and Guiraud, P. (2013). "Silica nanoparticles separation from water: Aggregation by cetyltrimethylammonium bromide (CTAB)." *Chemosphere*, 92(6), 681–687.

Minitab version 17.3.1 [Computer software]. Minitab, Inc., State College, PA.

Mortimer, M., Kasemets, K., and Kahru, A. (2010). "Toxicity of ZnO and CuO nanoparticles to ciliated protozoa *Tetrahymena thermophila*." *Toxicology*, 269(2–3), 182–189.

Piplai, T., Kumar, A., and Alappat, B. J. (2017). "Removal of mixture of ZnO and CuO nanoparticles (NPs) from water using activated carbon in batch kinetic studies." *Wat. Sci. Technol.*, 75(3–4), 928–943.

Rajagopalan, R., and Tien, C. (1976). "Trajectory analysis of deep-bed filtration with the sphere-in-cell porous media model." *AIChE J.*, 22(3), 523–533.

Shani, C., Weisbrod, N., and Yakirevich, A. (2008). "Colloid transport through saturated sand columns: Influence of physical and chemical surface properties on deposition." *Colloids Surf. A*, 316(1–3), 142–150.

Shen, C., Huang, Y., Li, B., and Jin, Y. (2010). "Predicting attachment efficiency of colloid deposition under unfavorable attachment conditions." *Water Resour. Res.*, 46(11), 1–12.

Shukla, A., Zhang, Y. H., Dubey, P., Margrave, J. L., and Shukla, S. S. (2002). "The role of sawdust in the removal of unwanted materials from water." *J. Hazard. Mater.*, 95(1–2), 137–152.

Sun, J. H., Dong, S. Y., Feng, J. L., Yin, X. J., and Xiao, C.-Z. (2011). "Enhanced sunlight photocatalytic performance of Sn-doped ZnO for methylene blue degradation." *J. Mol. Catal. A*, 335(1–2), 145–150.

Sun, Q., Li, Y., Tang, T., Yuan, Z., and Yu, C.-P. (2013). "Removal of silver nanoparticles by coagulation processes." *J. Hazard. Mater.*, 261, 414–420.

Tan, M., Qiu, G., and Ting, Y. P. (2015). "Effects of ZnO nanoparticles on wastewater treatment and their removal behavior in a membrane bioreactor." *Bioresour. Technol.*, 185, 125–133.

Torkzaban, S., Bradford, S. A., van Genuchten, M. T., and Walker, S. L. (2008). "Colloid transport in unsaturated porous media: The role of water content and ionic strength on particle straining." *J. Contam. Hydrol.*, 96(1–4), 113–127.

Tufenkji, N., and Elimelech, M. (2004). "Correlation equation for predicting single-collector efficiency in physicochemical filtration in saturated porous media." *Environ. Sci. Technol.*, 38(2), 529–536.

Westerhoff, P., Song, G., Hristovski, K., and Kiser, M. A. (2011). "Occurrence and removal of titanium at full scale wastewater treatment plants: Implications for TiO$_2$ nanomaterials." *J. Environ. Monit.*, 13(5), 1195–1203.

Xu, Z., Cai, J.-G., and Pan, B.-C. (2013). "Mathematically modeling fixed-bed adsorption in aqueous systems." *J. Zhejiang Univ.–Sci. A*, 14(3), 155–176.

Yao, K., Habibian, M. T., and O'Melia, C. R. (1971). "Water and wastewater filtration: Concepts and applications." *Environ. Sci. Technol.*, 5(11), 1105–1112.

Zeng, L. (2004). "Arsenic adsorption from aqueous solutions on Fe (III)-Si binary oxide adsorbent." *Water Q. Res. J. Can.*, 39(3), 267–275.